J. Biochem. 2009;146(2)231–240
doi:10.1093/jb/mvp062

The Presence of OMP Inclusion Bodies in a *Escherichia coli* K-12 Mutated Strain is not Related to Lipopolysaccharide Structure

M. Michela Corsaro[1], Ermenegilda Parrilli[1,2], Rosa Lanzetta[1], Teresa Naldi[1], Giuseppina Pieretti[1], Buko Lindner[3], Andrea Carpentieri[1], Michelangelo Parrilli[1] and M. Luisa Tutino[1,2,*]

[1]Dipartimento di Chimica Organica e Biochimica, Università di Napoli Federico II, Complesso Universitario Monte S. Angelo, Via Cintia 4, 80126 Napoli, Italy; [2]Facoltà di Scienze Biotecnologiche Università di Napoli Federico II, Complesso Universitario di Monte Sant'Angelo - Via Cinthia 80126 Napoli; and [3]Division of Immunochemistry, Research Center Borstel, Leibniz-Center for Medicine and Biosciences, Parkallee 10, D-23845 Borstel, Germany

Received March 30, 2009; accepted April 2, 2009; published online April 13, 2009

The role of lipopolysaccharides (LPSs) in the biogenesis of outer membrane proteins have been investigated in several studies. Some of these analyses showed that LPS is required for correct and efficient folding of outer membrane proteins; other studies support the idea of independence of outer membrane proteins biogenesis from LPS structure. In this article, we investigated the involvement of LPS structure in the anomalous aggregation of outer membrane proteins in a *E. coli* mutant strain (S17-1(λ*pir*)). To achieve this aim, the LPS structure of the mutant strain was carefully determined and compared with the *E. coli* K-12 one. It turned out that LPS of these two strains differs in the inner core for the absence of a heptose residue (HepIII). We demonstrated that this difference is due to a mutation in *waaQ*, a gene encoding the transferase for the branch heptose HepIII residue. The mutation was complemented to find out if the restoration of LPS structure influenced the observed outer membrane proteins aggregation. Data reported in this work demonstrated that, in *E. coli* S17-1(λ*pir*) there is no influence of LPS structure on the outer membrane proteins inclusion bodies formation.

Key words: *E. coli* S17-1 (λ*pir*), Fourier-transform mass spectrometry, inclusion bodies, LPS structures, NMR spectroscopy.

Abbreviations: DQF-COSY, double quantum filtered-correlation spectroscopy; GC-MS, gas chromatography-mass spectrometry; HMBC, heteronuclear multiple bond correlation; HSQC-DEPT, heteronuclear single quantum coherence-distortionless enhancement by polarization transfer; Kdo, 3-deoxy-D-*manno*-oct-2-ulosonic acid; ROESY, rotating-frame nuclear Overhauser effect spectroscopy; TOCSY, total correlation spectroscopy.

In Gram negative bacteria, the outer membrane proteins (OMPs) in order to reach the outer membrane (OM) must be translocated across the inner membrane and through the periplasmic space. All OMPs are synthesized with an N-terminal signal sequence that directs their transport across the inner membrane, this translocation occurs generally via the SecYEG translocon complex (*1*, *2*). These initial stages in the biogenesis of OMPs are well understood; however, the intermediate and late stages in OMP biogenesis are much less understood. Several observations suggest that the transport to and insertion into the outer membrane have to be facilitated and regulated processes. Indeed, due to their inherent hydrophobic nature, OMPs could be destined to fold prematurely and/or aggregate in the periplasm if not properly assisted during their transit towards the outer membrane (*3*). Several periplasmic proteins like Skp (*4*) or SurA (*5*) have been involved in OMPs biogenesis (*6*). Outer membrane folding factors have been also found out like an integral protein (Omp85) that functions as a general OMPs insertion machine (*7*, *8*).

In addition to proteins, lipids may play an important role in OMP biogenesis, not only because they provide the medium in which the OMPs insert to reach their native, but also for functional state. Lipopolysaccharide (LPS) and phospholipids have been considered by several authors as lipochaperones (*9*, *10*).

However, a final assessment on their role in OMPs biogenesis, especially for LPS molecules, is still largely controversial (*6*). The role of LPS might be to provide a scaffold for the protein to reach its final 3D arrangement, and in the maintenance of the native protein structure and its activity (*11*). For example, in *Escherichia coli* deep-rough mutants, the assembly of LamB and OmpF is kinetically retarded in the conversion between metastable trimer to stable native trimer (*11*). Furthermore, it is likely that specific interactions between OMPs and LPS within the outer membrane exist. For example, in the crystal structures of FhuA and OmpT an LPS molecule could be identified, indicating that specific binding sites exist for LPS on the native protein (*12*, *13*). De Cock, Tommassen and colleagues have studied the

*To whom correspondence should be addressed.
Tel: +39-081-674317, Fax: +39-081-674313,
E-mail: tutino@unina.it

role of LPS in the *in vitro* folding of the trimeric porin PhoE. They reported that LPS micelles promoted the formation of a folded PhoE monomer (*14*). The authors also demonstrated that LPS from deep-rough mutants is much less efficient in promoting folding (*14*), and that the negative charges in the inner core region are responsible for the ability of LPS to fold PhoE (*15*). LPS has also been shown to be involved in the *in vitro* folding of OmpA in combination with Skp into phospholipid vesicles (*16*).

One major caveat in the interpretation of *in vitro* experiments is that the late stages in the biogenesis of LPS itself are elusive. Extending to the cell the conclusions deriving from the *in vitro* experiments would necessary imply that LPS and OMPs intermediates interact in the periplasm before insertion of both components into the outer membrane. In contrast to this latter conclusion, it has been reported the identification of two independent proteinaceous outer membrane insertion machineries, each one specific for OMPs (Omp85) (*7*) and LPS (Imp) (*17*). This situation suggests that the outer membrane insertion of these components take place separately, and therefore OMPs and LPS could not encounter in the periplasm. Moreover, the disruption of the *Nesseiria meningitidis lpxA* gene, which encodes the first enzyme in LPS biosynthesis, resulted in the construction of mutant strains that are completely devoid of LPS. In these mutants, expression and assembly of OMPs was largely unaffected, showing that LPS does not have an obligatory role in the biogenesis of OMPs at least in this organism (*18*).

In this article, we investigated on the LPS structure involvement in OMPs anomalous aggregation in a *E. coli* mutant strain (S17-1(λ*pir*)). To achieve this aim, the LPS structure of the mutant strain was determined and compared with that of *E. coli* K-12. It turned out that LPS of this two strains differs in the inner core for the absence of a heptose residue (HepIII). We demonstrated that the observed phenotype is due to a mutation of *waaQ* gene (*19*), coding for a transferase for the branch heptose HepIII residue. *waaQ* Mutation was complemented to find out if the restoration of LPS structure influenced the observed OMPs aggregation.

MATERIAL AND METHODS

Microbiology and Molecular Biology Methodologies—*Escherichia coli* cells were routinely grown in aerobic conditions at 37°C in Terrific broth (*20*) containing 100 μg/ml of ampicillin or if transformed. Genetic manipulations were carried out as previously described (*20*). *Escherichia coli* DNA genomic purification was performed by ChargeSwitch gDNA Mini Bacteria Kit (Invirtogen). All PCR amplifications were performed as previously described (*20*). The amplified fragments were cloned and their nucleotide sequences checked to rule out the occurrence of mutations during synthesis.

Protein Inclusion Bodies Extraction—The cell pellet coming from 200 ml culture was resuspended in 10 ml of 50 mM Tris–Cl, 1 mM EDTA, 1 mM PMSF pH 8.0 and lysozyme was added at 1 mg/ml. After 30 min of incubation on ice, 5.5 ml of lysis solution (50 mM Tris–Cl, 2% Triton X-100, 63 mM EDTA, pH 8.0) were added and the mixture was stirred for 15 min at 4°C. The cell breaking was enhanced by six cycles of sonication (30 s on, 1 min off) on ice, (Branson sonicator, model B-15, intensity 4.5). The sample was centrifuged at 2,000*g*, 4°C, for 20 min and the pellet was resuspended in 10 ml of 50 mM Tris–Cl, 1 mM EDTA, pH 8, divided in aliquots of 1 ml and centrifuged at 1,800*g*, 4°C, for 20 min. This wash was repeated twice and the inclusion bodies were lastly dried by a centrifugation step of 5 min at 9,500*g*, 4°C, and stored as dry pellets at 4°C.

Protein SDS Analysis—Protein samples for SDS–PAGEwere prepared and separated on SDS-containing polyacrylamide (12%) gels using standard methods (*20*).

LPS Isolation—The LPSs were extracted from dry cells by the phenol/chloroform/light petroleum ether method (*21*). The yield was 3.2% of the bacterial dry mass for both *E. coli* S17-1 (λ*pir*) and *E. coli* S17-1(λ*pir*)-pUC*waaQ*.

Preparation of OS and waaQ-OS Fractions—A fraction of *E. coli* S17-1 (λ*pir*) LPS was totally delipidated as reported (*21*). Briefly, 40 mg of LPS were stirred in anhydrous hydrazine (2 ml) at 37°C for 90 min. After usual work up the sample (33 mg) was treated with 5 ml of 4 M KOH for 16 h at 120°C. The phosphorylated oligosaccharides were purified from salts by gel-filtration chromatography on a Sephadex G10 column (Pharmacia, 1.5×47 cm, H_2O as eluant, flow rate 21 ml/h), giving after lyophilization a residue of 16 mg of OS fraction. A sample (30 mg) of *E. coli* S17-1(λ*pir*)-pUC*waaQ* LPS was treated in the same way, obtaining 9 mg of *waaQ*-OS fraction.

Analytical Methods—LPSs (1 mg each of the *E. coli* S17-1(λ*pir*) and *E. coli* S17-1(λ*pir*)-pUC*waaQ* strains) were dried over P_2O_5 overnight and treated with 1M HCl/CH_3OH (1 ml) at 80°C for 20 h, to analyse both glycosyl and fatty acids composition. The crude reaction for both samples was extracted twice with hexane; the two extracts were pooled, dried under a stream of air and treated with acetic anhydride (100 μl) at 100°C for 15 min. The methanol layer for both samples was neutralized with Ag_2CO_3, dried and acetylated. All the samples were injected into the Gas Chromatography-Mass Spectrometry (GC-MS), acetylated fatty acids methylesters were recovered in the hexane phase, whereas the methylglycoside derivatives were in the methanolic one.

For methylation analysis, the OS and the *waaQ*-OS fractions (1 mg each) were first de-phosphorylated with 48% HF at 4°C for 16 h and then N-acetylated by dissolving in dry methanol and treating them with 50 μl of acetic anhydride for 16 h. After evaporation of the solvents the samples were separately methylated as reported (*22*). Linkage analysis was performed as follows: the methylated samples were carboxymethyl reduced with lithium triethylborohydride (Aldrich), mild hydrolyzed to cleave ketosidic linkage, reduced by means of NaBD4, then totally hydrolyzed, reduced with NaBD4 and finally acetylated as described (*23*).

For absolute configuration determination a sample of *E. coli* S17-1(λ*pir*), LPS (2 mg) was hydrolysed with a mixture of 2 M H_2SO_4/AcOH and derivatized as acetylated octyl glycosides (*24*). The sample was analysed by GC-MS.

GC-MS Analysis—Methyl glycoside acetates were analyzed on a 6850A Gas Chromatograph equipped with an Agilent Technologies 5973N MS instrument and a Zebron ZB-5 capillary column (Phenomenex, 30 m × 0.25 mm i.d., flow rate 1 ml/min, He as carrier gas). Acetylated methyl glycosides analysis was performed with the following temperature program: 150° for 5 min, 150°→250° at 3°/min, 250° for 10 min. Acetylated methyl esters fatty acids analysis was performed as follows: 150° for 3 min, 150°→280° at 10°/min, 280° for 15 min. For partially methylated alditol acetates the temperature program was: 90°C for 1 min, 90°C →140°C at 25°C/min, 140°C→200°C at 5°C/min, 200°C →280°C at 10°C/min, 280°C for 10 min. Analysis of acetylated octyl glycosides was performed as follows: 150°C for 5 min, 150°C→240°C at 6°C/min, 240°C for 5 min.

NMR Spectroscopy—Spectra were recorded on a Varian Inova 500 spectrometer equipped with a reverse probe at 300 K. ^{13}C and ^{1}H chemical shifts were measured in D_2O using acetone, at δ 2.225 and 31.4 for proton and carbon, respectively, as internal standard. Two-dimensional homo- and heteronuclear experiments (DQF-COSY, TOCSY, ROESY, $^{1}H,^{13}C$-HSQC–DEPT and HMBC) were performed using standard pulse sequences available in the Varian software. $^{1}H,^{31}P$-HSQC experiments were recorded on a Bruker DRX-400 spectrometer, using aqueous 85% phosphoric acid as external reference (0.00 p.p.m.).

Mass Spectrometry Analysis—Electrospray ionization Fourier transform mass spectrometry (ESI FTMS) of oligosaccharides was performed in the negative ion mode using an APEX Qe Instrument (Bruker Daltonics, USA) equipped with a 7 Tesla magnet and an Dual Apollo ion source. Samples (~10 ng/μl) were dissolved in a 50:50:0.001 (v/v) 2-propanol–water–triethylamine mixture and sprayed at a flow rate of 2 μl/min. Capillary entrance voltage was set to 3.8 kV and drying gas temperature to 170°C. Mass scale calibration of the broadband spectra was performed externally with a similar compound of known structure. The spectra were charge deconvoluted and mass numbers given refer to monoisotopic masses of the neutral molecule.

RESULTS

*Escherichia coli S17-1(*λpir*) Cells Contain OMP Inclusion Bodies*—The protocol usually employed to isolate inclusion bodies (*25*) (see MATERIAL AND METHODS section) was applied on *E. coli* S17-1(λ*pir*) cells (*26–28*) during an analysis not related with the experiments reported in this article. The insoluble protein fraction was subjected to SDS–PAGE analysis and results are shown in Fig. 1 (lane 1). The electrophoretic separation revealed the presence of two main bands corresponding to proteins with an apparent molecular mass of about 37 kDa. N-terminal protein sequencing was used to identify the two proteins; the upper band resulted to be OmpA protein (*29*), while the lower band turned out to be made by OmpF (*30*) and OmpC (*31*) proteins. Furthermore, all proteins were lacking in signal peptide sequence indicating that they were processed by the SecYEG translocon complex (*1*). The upper band in

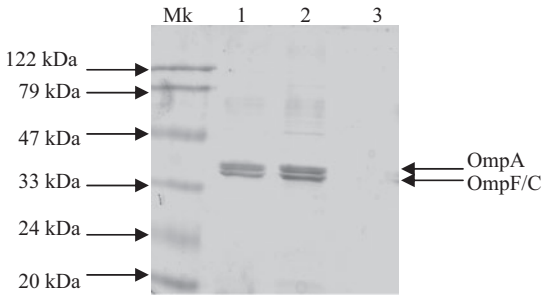

Fig. 1. **SDS analysis of *E. coli* S17-1(λ*pir*) inclusions bodies.** SDS analysis of samples obtained by appling the protocol to inclusion bodies isolation to *E. coli* S17-1(λ*pir*) (Lane 1), *E. coli* S17-1(λ*pir*)-pUC*waaQ* (Lane 2) and *E. coli* K-12 (Lane 3) cells.

Fig. 1 corresponds to OmpA, and its electrophoretic mobility is in perfect agreement with previous reports (*17*). The lower band contains two proteins with almost coincident apparent molecular mass: OmpC and OmpF. The two proteins are porins, which are reported to be resistant to heat denaturation and detergent solubilization, provided that they are properly assembled (*32*). For instance, *E. coli* OmpF is a trimeric protein that remains folded in presence of SDS, and that dissociates at least to the dimeric form when it is heated prior to SDS–PAGE analysis (*33–36*). As shown in Fig. 1, the SDS gel analysis revealed the presence of OmpC and OmpF in a band displaying the electrophoretic mobility of the monomeric form. These results indicated that the periplasmatic aggregates, isolated from *E. coli* S17-1(λ*pir*) cells, contain OmpF and OmpC in a not properly assembled fold.

*LPS Structure of E. coli S17-1 (*λ*pir)*—LPSs were isolated from *E. coli* S17-1 (λ*pir*) cells by the PCP method (*21*). The yield was 3.2%. Glycosyl analysis together with absolute configuration determination showed the presence of D-galactose, D-glucose, D-glucosamine, L-*glycero*- D-*manno*-heptose and Kdo. According to lipid composition for an *E. coli* strain (*37*), GC-MS analysis identified the presence of C12:0, C14:0, and C14:0 (3-OH). LPS was then completely deacylated by degradation under alkaline conditions and purified by gel filtration chromatography, obtaining the OS fraction.

Methylation analysis showed the presence of *t*-Gal, *t*-Glc, 2-Glc, 6-Glc, 3,6-Glc, *t*-Hep, 3-Hep, *t*-Kdo, 4,5-Kdo and traces of 4-linked Kdo units.

The negative ions ESI FT-ICR mass spectrum (Fig. 2) showed many mass peaks in the region between 1,800 u and 2,500 u, suggesting the presence of a complex mixture of phosphorylated oligosaccharides. Taking into account the glycosyl analysis, most peaks were identified as reported in Table 1. The molecular peak at 2,244.566 u was attributed to molecular species (glycoform I) containing two GlcN, three Hep, four Hex, two Kdo units and three phosphate groups, according to the calculated molecular mass of 2,244.562 u. A shift of 354 u, indicative for the loss of one hexose and one heptose, identified the mass peak at 1,890.452 u as glycoform II. Finally, the peak at 2,110.510 u can account for the presence of glycoform III, which was consistent with a composition of two HexN, two Hep, three Hex, three Kdo units and three

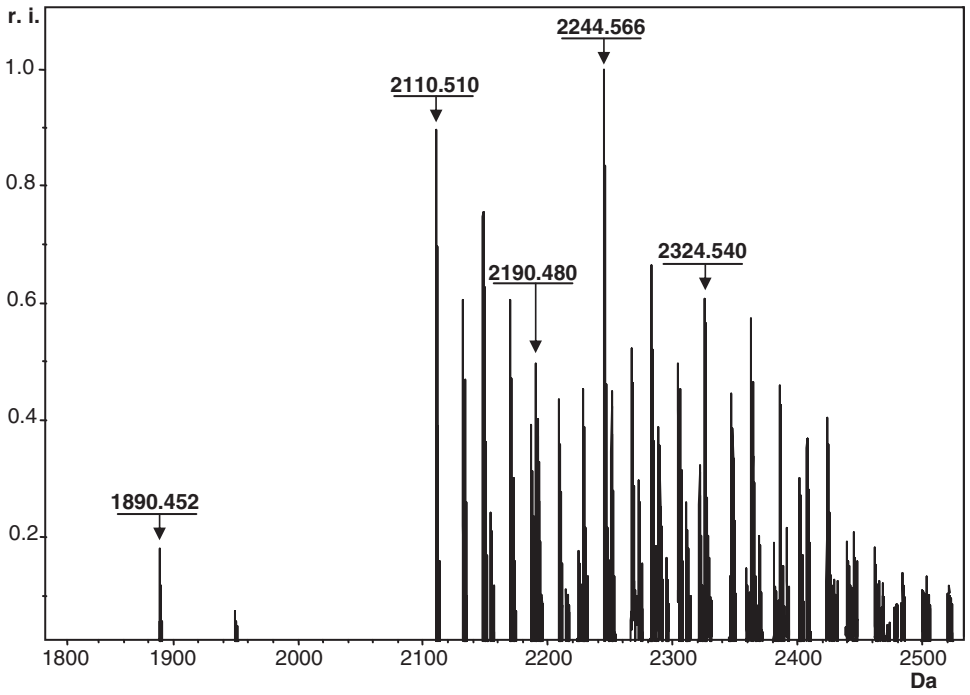

Fig. 2. **Charge deconvoluted ESI FT-ICR mass spectrum of the fully de-acylated LPS from *E. coli* S17-1(λ*pir*).** The spectrum was acquired in negative ion mode. Mass numbers given refer to monoisotopic peak of the neutral molecular species. Peaks not assigned belong to sodium and potassium adducts.

Table 1. **Composition of the main species present in the ESI FT-ICR mass spectrum of the *E. coli* S17-1(λ*pir*) OS fraction.**

Glycoform	Observed Mass u	Calculated Mass u	Composition
I	2244.566	2244.562	$Hex_4Hep_3Kdo_2HexN_2P_3$
	2324.540	2324.532	$Hex_4Hep_3Kdo_2HexN_2P_4$
II	1890.452	1890.449	$Hex_3Hep_2Kdo_2HexN_2P_3$
III	2110.510	2110.507	$Hex_3Hep_2Kdo_3HexN_2P_3$
	2190.480	2190.474	$Hex_3Hep_2Kdo_3HexN_2P_4$

phosphate groups. Thus the ESI FT-ICR mass spectrum indicated the presence of three main glycoforms, which differed in glycosyl composition. Glycoforms I and III were also present as tetra-phosphorylated species as demonstrated by the presence of 2,324.54 u and 2,190.48 u, respectively.

The complete assignment of the proton and carbon chemical shifts of OS fraction was obtained on the basis of the DQF-COSY, TOCSY, ROESY, $^{1}H,^{13}C$-HSQC–DEPT, $^{1}H,^{13}C$-HSQC and HMBC, and $^{1}H,^{31}P$-HSQC spectra (Tables 2 and 3). In the ^{1}H NMR spectrum (Fig. 3), all the anomeric signals (indicated by letters **A**–**N**, according to decreasing proton chemical shifts) were assigned to α-configurated monosaccharides, on the basis of the low value of the $^{3}J_{H1,H2}$ coupling constants, except for the signal at δ 4.81 ($^{3}J_{H1,H2}$ 7.8 Hz), which belongs to the distal β-GlcN unit of the lipid A moiety. All linkage positions were substantiated by downfield glycosylation shift of substituted carbons. Residues **A** (H1 = δ 5.71, $^{3}J_{H1,H2}$ = 3.3 Hz, $^{3}J_{H,P}$ = 6.6 Hz) and **N** (H1 = δ 4.81, $^{3}J_{H1,H2}$ = 7.8 Hz) were recognized as the vicinal and distal glucosamine of the lipid A, respectively, because their H2 protons were correlated to nitrogen bearing carbons at δ 55.3 and δ 56.5, respectively. Moreover a NOE contact between the proton anomeric signal of **N** and protons H-6 of **A** (Table 3) revealed that these residues were 1→6 connected.

The residue **B** was *gluco* configurated, on the basis of the high value of the ring proton coupling constants, and it was assigned to a 2-substituted glucose due to the downfield shift of its C2 compared with an unsubstituted glucose (*38*). A strong NOE contact between **G** residue anomeric proton at δ 5.16 and both H1 and H2 of **B** (Table 3) indicated that **G** was linked to the position 2 of **B**. In addition in the ROESY experiment the H1 **B** signal showed a NOE contact with H3 of **D** at δ 3.88. Since the residue **G** was identified as α-6-substituted glucose and residue **D** was identified as 3,6-substituted glucose, the trisaccharide sequence→6)-Glc-(1→2)-Glc(1→3)-Glc was recognized. Three spin systems **H**, **F** and **M** were recognized to be heptoses on the basis of the low $^{3}J_{H1,H2}$ and $^{3}J_{H2,H3}$ values. In addition the downfield of C3 chemical shifts for **H** and **F** at 80.6 p.p.m. suggested that both were 3-substituted. According to a NOE contact between the anomeric proton of the residue **H** and H3 of residue **F** the sequence Hep-(1→3)-Hep was recognized. Heptose **H** was in turn substituted at O-3 position by glucose **D**, as deduced from a NOE cross peak between H1 **D** and H3 **H**. Considering the ^{13}C chemical shifts of unsubstituted heptose the residue **M** was assigned to a terminal heptose connected to the O-6 position of glucose **G**, as shown by the NOE contact between its anomeric proton and one of the H6 protons

Table 2. **^{1}H and ^{13}C NMR chemical shifts (ppm) of the oligosaccharides obtained from *E. coli* S17-1(λ*pir*) OS fraction.**

Glycoform	residue		H1	H2/3ax	H3/3eq	H4	H5	H6a	H6b/7a	H7b/8a	H8b
			C1	C2	C3	C4	C5	C6	C7	C8	
I, II, III	**A**	6-α-GlcN 1P	5.71	3.44	3.90	3.62	4.11	4.29	3.79		
			92.1	55.3	70.4	70.6	73.5	70.2			
I	**B**	2-α-Glc	5.44	3.67	3.81	3.52	4.06	3.83	3.83		
			97.8	76.5	71.5	70.2	72.2	61.2			
II, III	**C**	*t*-α-Glc	5.38	3.70	3.75.	3.42	4.03	3.75	3.75		
			97.2	73.2	n.d	70.6	72.2	62.0			
I	**D**	3,6-α-Glc	5.27	3.65	3.88	3.76	4.13	4.06	3.77		
			101.7	71.2	81.9	73.1	71.6	66.2	3.77		
II, III	**E**	3,6-α-Glc	5.26	3.69	3.92	3.83	4.11	4.08			
			101.7	72.0	81.9	n.d.	71.6	66.2			
I, II, III	**F**	3-α-Hep 4P	5.25	4.14	4.08	4.45	4.28	n.d.	3.70		
			99.8	71.6	80.6	71.5	n.d.		64.0		
I	**G**	6-α-Glc	5.16	3.59	3.73	3.49	4.11	3.91	3.67		
			96.8	72.4	n.d.	70.2	71.1	65.8			
I, II, III	**H**	3-α-Hep 4P	5.15	4.37	4.05	4.35	3.71	4.08	3.85		
			103.1	70.3	80.6	70.3	n.d.	69.9	63.7		
I	**I**	*t*-α-Gal	4.99	3.81	4.00	4.02	3.72	3.95	4.08		
			99.1	69.5	70.3	69.9	71.8	n.d.	62.0		
II, III	**L**	*t*-α-Gal	4.96	3.83	4.00	4.03	3.72	3.89	4.08		
			99.1	69.5	70.3	69.9	71.8	n.d.	62.0		
I	**M**	*t*-α-Hep	4.88	3.97	3.81	3.84	3.59	4.01	3.70		
			100.3	70.4	71.5	67.2	70.5	n.d.	64.0		
I, II, III	**N**	6-β-GlcN 4P	4.81	3.09	3.85	3.68	3.74	3.42	3.85		
			100.3	56.5	n.d.	76.4	n.d.	63.4			
I, II, III	**O**	4,5-Kdo	n.d.	2.07	1.77	4.12	4.25	n.d.	n.d.	n.d.	n.d.
				n.d.	35.4	71.6	70.3				
I, II, III	**Q**	*t*-Kdo	n.d.	2.19	1.75	4.09	4.23	n.d.	n.d.	n.d.	n.d.
				35.5		67.1	n.d				

Table 3. **Inter-residue NOE connectivities from the anomeric protons of the *E. coli* S17-1(λ*pir*) OS fraction.**

Residue	Inter-residue
B	H1 of **G**, H3 of **D**
C	H3 of **E**
D	H3 of **H**
E	H3 of **H**
F	H5 of **O**
G	H1, H2 of **B**
H	H3 of **F**
I	H6a,b of **D**
L	H6a of **E**
M	H6a of **G**
N	H6a,b of **A**

of **G**. By exclusion, the residue **I** was assigned to a galactose connected at O-6 position of **D**, according to NOE connectivities measured between the anomeric proton of **I** and both H6 protons of **D**. As for the signals of the Kdo units only the connectivities H3-H5 were identified due to the overlapping with other signals. In any case the presence of the disaccharide α-Kdo-(2→4)-α-Kdo was inferred from methylation data and the linkage between the heptose **F** and the position 5 of the 4,5-linked Kdo unit was deduced from a NOE cross peak between the anomeric proton of **F** and a signal at δ 4.25, attributed to H5 of the Kdo unit **O**. All the inter-glycosidic linkages were inferred by scalar hetero-correlation among the anomeric protons and the corresponding glycosylated carbons by a HMBC experiment.

The degree of phosphorylation was established on the basis of the ESI FT-ICR mass spectrum of this fraction (Fig. 2), which revealed the presence of glycoform I and III as tetra- and tri-phosphorylated oligosaccharides and glycoform II as a triphosphorylated oligosaccharide.

The localization of phosphate groups was inferred by a ^{1}H,^{31}P-HSQC, that showed correlations of ^{31}P signals at 1.05 and 1.64 p.p.m. with H1 **A** and H4 **N**, respectively, and 2.44 p.p.m. with both H4 **F** and H4 **H**. As the OS fraction was analysed as a mixture it was not possible to assign the precise phosphate group position for each single molecular species. However, it is possible to assume that the missing phosphate is that at the O-4 position of glucosamine II (*39*).

These data indicated for the *E. coli* S17-1 (λ*pir)* LPS the following main structure:

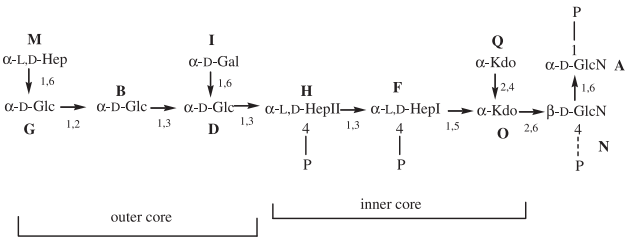

Glycoform I

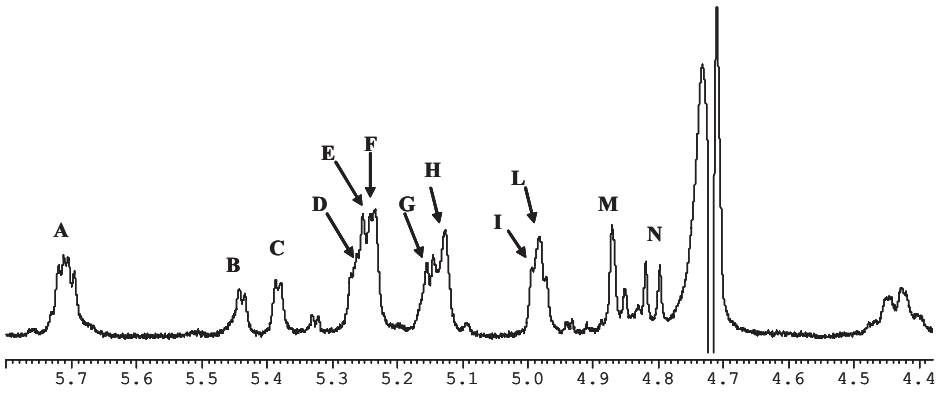

Fig. 3. **^{1}H-NMR anomeric region of the fully de-acylated LPS from *E. coli* S17-1(λ*pir*).** ^{1}H-NMR anomeric region of the fully de-acylated LPS from *E. coli* S17-1(λ*pir*) performed at 300 K. The spectrum was recorded in D_2O at 500 MHz. The letters refer to the residues as described in Table 2.

ESI FT-ICR data revealed the presence of other two glycoforms (Table 1). Glycoform II contained one less heptose and hexose residues in the outer core structure respect to glycoform I. In addition glycoform III contained one more Kdo unit in the inner core. Glycoform II structure was inferred from the identification of a terminal glucose residue in the methylation analysis, together with the presence in NMR experiments of residue **C**, that was attributed to an unsubstituted α-glucose. A NOE cross-peak (Table 3) between H1 of **C** and H3 of **E** was consistent with the disaccharide structure α-Glc-(1→3)-Glc, linked in turn to the inner core structure.

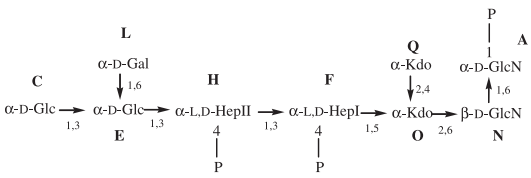

Glycoform II

Finally, glycoform III, in agreement with methylation data, which revealed the presence of 4-substituted Kdo units, was suggested to be:

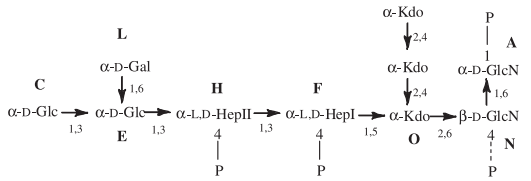

Glycoform III

Finding of waaQ Gene Mutation—The structural investigation of lipopolysaccharide of *E. coli* S17-1(λ*pir*) demonstrated that it differs from *E. coli* K-12 LPS one (*39*) for the absence of the inner core HepIII. Since *E. coli* S17-1(λ*pir*) is an engineered strain derived from *E. coli* K-12 (*26–28*), the reported difference in LPS structure could be due to a not yet described mutation in gene (*waaQ)* encoding the transferase for the branch HepIII residue (*19*). To verify this hypothesis, the sequence of *waaQ* gene of *E. coli* S17-1(λ*pir*) was analysed. The analysis was performed by PCR using several primers (Table 4) designed to amplify different regions of *waaQ* gene, and all PCR products obtained were sequenced. The DNA sequence analysis demonstrated the presence of a 830 bp long insertion in *waaQ* coding sequence occurred between nucleotide 918 and nucleotide 919. Inserted sequence resulted to encode a portion of transposase TnpA (from amino acid 19 to amino acid 295) (*40*).

Cloning and Expression of waaQ gene for Complementation—In order to complement the *waaQ* gene mutation the pUC*waaQ* vector was constructed. w*aaQ* Gene was amplified by PCR using the genomic DNA extracted from *E. coli* K-12 cells as template. The primers (WaaQProm and WaaQErv) were designed to amplify *waaQ* gene and its promoter region (*41*) and to introduce *XbaI* and *EcoRI* restriction sites. The PCR product was subjected to a double *XbaI* and *EcoRI* digestion and inserted into pUC18 corresponding sites, generating pUC*waaQ*. *E. coli* S17-1(λ*pir*) were transformed with pUC*waaQ* and recombinant cells were grown as reported in MATERIAL AND METHODS section.

LPS Structure of Complemented E. coli S17-1(λpir) Strain—LPS was extracted from *E. coli* S17-1(λ*pir*)-pUC*waaQ* recombinant cells with the PCP method. In order to compare the obtained results with those of the OS fraction from wild type cells, the LPS fraction was completely de-acylated (*waaQ*-OS fraction) and the structure determined by ESI FT-ICR MS, methylation analysis and NMR experiments. The comparison of the negative ions mass spectrum of *waaQ*-OS fraction (Fig. 4, Table 5) with that of OS fraction (Fig. 2, Table 1) revealed that each glycoform contained one additional heptose unit. Moreover the mass peaks at 2,596.573 u and 2,242.454 u indicated that glycoforms I and II presented additional phosphate groups.

Methylation analysis of the *waaQ*-OS fraction showed the presence of one further residue, that was identified as a 3,7-substituted heptose, and the relative ratio of *t*-Gal:3-Hep:3,7-Hep was 1:0.9:0.8 whereas *t*-Gal:3-Hep was 1:1.9 in the OS fraction. The NMR analysis revealed additional anomeric proton and carbon signals at 5.00 and 101.6 p.p.m., respectively (Fig. 5), and a methylene

Table 4. **Bacterial strains, plasmids and oligonucleotides used in this work.**

	Description	Reference
Bacterial strains		
S17-1(λ*pir*)	*Escherichia. coli* strain S17-1(λ*pir*) [*thi, pro, hsd* (r^- m^+) *recA*::RP4-2-TC^r:: Mu Km^r::Tn7 Tp^r Sm^r λ*pir*]	(*26–28*)
Plasmids		
pUC18	Ap^r; *α-lac*/MCS^a	(*42*)
pUC*waaQ*	pUC18 containing the *waaQ* gene	This paper
Oligonucleotides		
WaaQErv	5′- AAGAATTCTCATAATTGTGCATTCCTG-3′	
WaaQProm	5′- TTTCTAGACGGGTCGGATTGCTGC-3′	
WaaQGErv	5′- AAGAATTCGCGGCAACTGTTGATGC-3′	
WaaQ1fw	5′- TCCTTGAGCCATTAGGTATTACCG-3′	
Oligo tnprv	5′- TACAATAGAATTTGGCATGAGATTGG-3′	

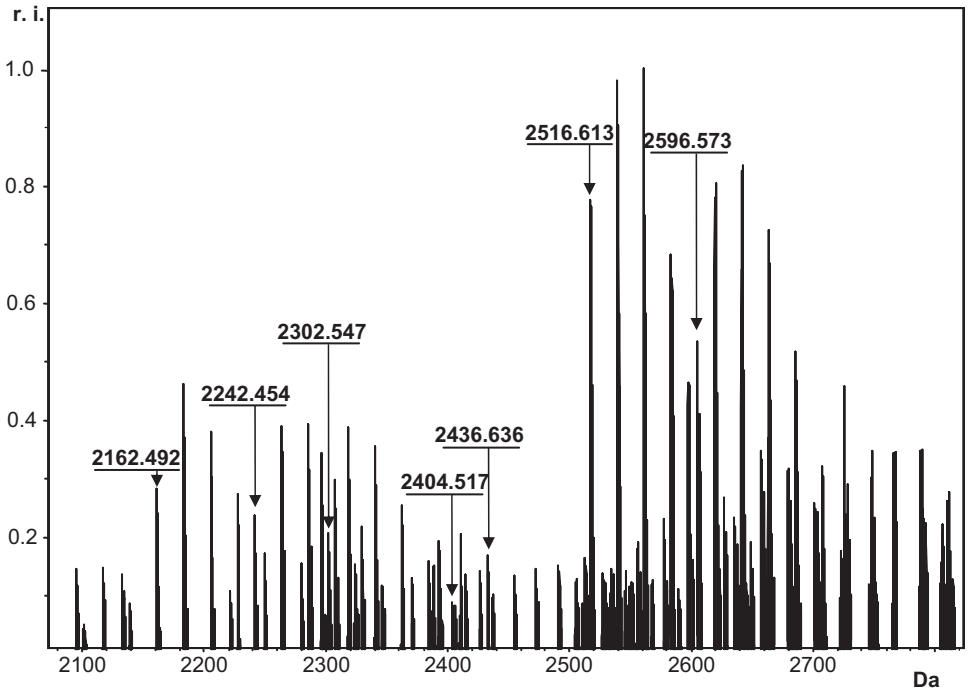

Fig. 4. **Charge deconvoluted ESI FT-ICR mass spectrum of the fully de-acylated LPS from *waaQ* complemented *E. coli* S17-1(λ*pir*).** The spectrum was acquired in negative ion mode. Mass numbers given refer to monoisotopic peak of the neutral molecular species. Peaks not assigned explicitly belong to sodium and potassium adducts.

Table 5. **Composition of the main species present in the ESI FT-ICR mass spectrum of the *E. coli* waaQ-OS fraction.**

Glycoform	Observed Mass u	Calculated Mass u	Composition
I	2436.636	2436.625	$Hex_4Hep_4Kdo_2HexN_2P_3$
	2516.613	2516.591	$Hex_4Hep_4Kdo_2HexN_2P_4$
	2596.573	2596.557	$Hex_4Hep_4Kdo_2HexN_2P_5$
II	2162.492	2162.476	$Hex_3Hep_3Kdo_2HexN_2P_4$
	2242.454	2242.442	$Hex_3Hep_3Kdo_2HexN_2P_5$
III	2302.547	2302.568	$Hex_3Hep_3Kdo_3HexN_2P_3$
	2404.517	2404.516	$Hex_3Hep_3Kdo_3HexN_2P_4{}^*Na$

carbon signal shifted at 70.2 p.p.m. These signals were compatible with the disaccharide fragment α-Hep(III)-(1→7)-α-Hep(II) of the inner core and were in agreement with the K-12 inner core structure (*39*). The non-coincidence of the chemical shifts of anomeric protons (<±0.06 p.p.m.) of the *waaQ*-OS fraction with that of *E. coli* S17-1(λ*pir*) OS can be explained with a different content of each glycoform and with a different phosphorylation degree. All these structural data indicated the successful complementation of *waaQ* mutation in *E. coli* S17-1(λ*pir*).

Outer Membrane OMP Inclusion Bodies in E. coli S17-1(λpir) Complemented Strain—In order to find out

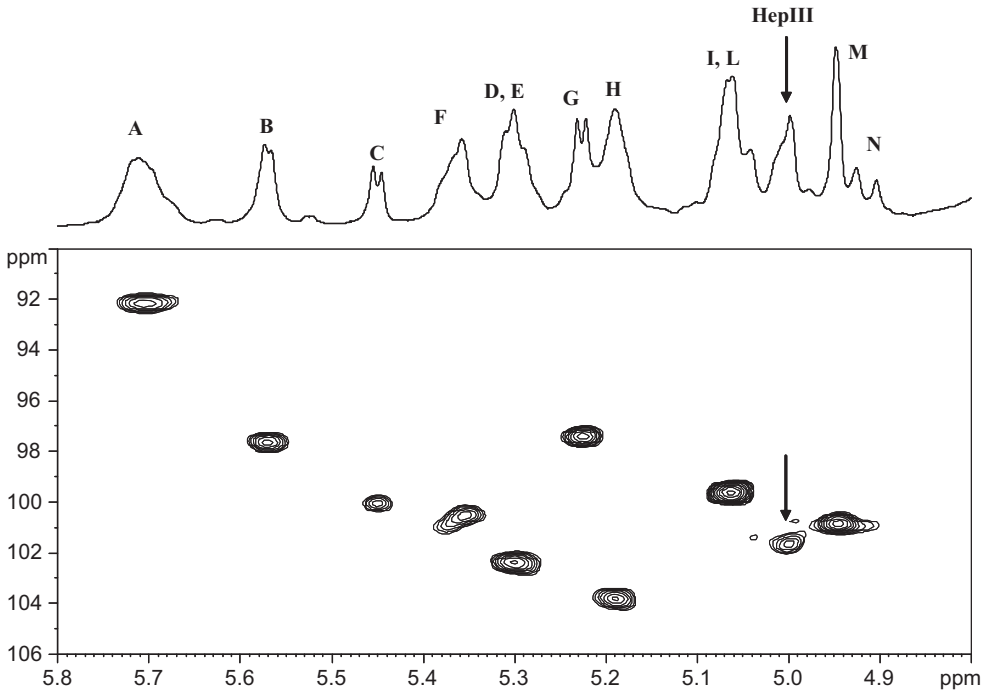

Fig. 5. **^{1}H,^{13}C-HSQC spectrum of the fulled de-acylated LPS from *waaQ* complemented *E. coli* S17-1(λ*pir*).** Anomeric region of the ^{1}H,^{13}C-DEPT-HSQC spectrum of the fully de-acylated LPS from waaQ complemented *E. coli* S17-1(λ*pir*) performed at 500 MHz in D_2O at 300 K. The letters refer to the residues as described in Table 2. The anomeric ^{1}H/^{13}C correlation of HepIII is indicated by arrow.

if the restoration of LPS structure influenced the aggregation of OMPs, the *E. coli* S17-1(λ*pir*)-pUC*waaQ* cells were subjected to inclusion bodies extraction protocol and resulting insoluble matter analysed. The electrophoresis analysis (Fig. 1, lane 2) revealed that the sample contains the same bands as recovered in the analysis of *E. coli* S17-1(λ*pir*) inclusion bodies, demonstrating that there was no difference between *E. coli* S17-1(λ*pir*)-pUC*waaQ* and *E. coli* S17-1(λ*pir*) in OMP's aggregation tendency.

DISCUSSION

The role of LPS in the biogenesis of OMPs have been investigated in several studies (*6*). These analyses, mainly performed by *in vitro* folding studies, showed that LPS is required for correct and efficient folding of OMPs and that LPS influences the correct oligomerization of OMPs, such as OmpF protein (*32*). Since we observed that in a *E. coli* strain OMPs are inclined to form aggregates, we decided to investigate the influence of LPS structure on this abnormal phenomenon.

OMPs anomalous aggregates from *E. coli* S17-1(λ*pir*) cells (*26–28*) were recovered by applying the protocol for isolation of inclusion bodies. Retrieved material consisted mainly of OmpA, OmpF and OmpC (Fig. 1), and reported results indicates that the periplasmatic aggregates, isolated from *E. coli* S17-1(λ*pir*) cells, contain OmpF and OmpC in a not properly assembled fold. If all the synthesized OmpF, OmpC and OmpA molecules would aggregate, *E. coli* S17-1(λ*pir*) should have displayed a severe reduction of cell viability. Therefore, growth profiles of *E. coli* S17-1(λ*pir*) and *E. coli* K-12 (which is its best characterized closest ancestor) were compared, and they resulted to be quite superimposable (data not shown). This result indicates that the OMPs aggregation involved only a small fraction of OMPs synthesized by the cell. The above observation suggests that if a mutation arose in *E. coli* S17-1(λ*pir*) it does not involved a pleiotropic gene, such as Omp85 (*8*), in OMPs biogenesis. Since our data demonstrate that the three proteins were correctly translocated across the inner membrane in the periplasmic compartment, the folding problems likely occur during some late stage in OMP biogenesis, *i.e*. protection and transport in the periplasm and insertion into the outer membrane. Therefore, our attention was focused on the LPS structure involvement in the formation of the anomalous OMPs aggregates. Structural determination of LPS from *E. coli* S17-1(λ*pir*) demonstrated that it differs from *E. coli* K-12 LPS only in the absence of the inner core HepIII, this difference being observed in all the glycoforms isolated. Interestingly, in a previous paper (*19*) describing the LPS structure of a *E. coli* R1 mutant, the lack of phosphorylation on Hep II was correlated to the absence of Hep III. In the *E. coli* S17-1(λ*pir*) LPS, the absence of Hep III is compatible with the Hep II phosphorylation.

Looking at the LPS biosynthetic pathway in *E. coli*, the lack of HepIII residue can be related to the inactivation of the heptose transferase encoded by *waaQ* gene. *E. coli* S17-1(λ*pir*) *waaQ* gene resulted to be knocked out by the insertion of a DNA fragment coding for a portion of TnpA transposase (*40*). This not previously described mutation could be a heritage of different cycles of mutagenesis

used to generate *E. coli* S17-1(λ*pir*) strain (*26–28*). Although the insertion destroys *waaQ* coding frame, it allows the *waa* operon (*41*) transcription and the expression of downstream *waa* genes, as inferred by *E. coli* S17-1(λ*pir*) LPS structure determination. *waaQ* Mutation was then complemented by constructing the recombinant *E. coli* S17-1(λ*pir*)-pUC*waaQ* strain. The complementation experiment was carried out by supplying a wild-type *waaQ* gene to the *E. coli* S17-1(λ*pir*) mutant strain, which chromosome contains a non-functional *waaQ* gene copy. As demonstrated by Whitfield and coworkers (*19*) WaaQ protein is the specific transferase responsible for the branch HepIII residue addition to the oligosaccharide backbone. Therefore, as far the oligosaccharide fraction is concerned, only two possible LPS types could have been recovered from *E. coli waaQ* complemented strain: (i) LPS still lacking of HepIII (in the case of not successful genetic complementation), or (ii) LPS containing HepIII residue (in the case of successful genetic complementation).

Since the in depth structural analysis of complemented LPS is not an objective of the present study we decided to carry over our analyses on the oligosaccharide mixtures. The LPS from the recombinant strain resulted to be identical to the *E. coli* K-12 one. The first suggestion of the occurred heptose insertion came from the comparison of *waaQ*-OS MS data with that of OS fraction, as all the glycoforms were present with an additional heptose. The position of the heptose incorporation was clearly indicated from NMR analysis and strongly supported by the methylation data. Even though the NMR analysis was performed on a mixture of oligosaccharides, the simultaneous appearing of new signals attributed to an additional heptose together with the 'glycosylation shift' of a methylene carbon signal was distinctly displayed in the ^{1}H and ^{1}H,^{13}C-HSQC experiments. The quantitative methylation analysis performed on both OS and waaQ-OS fractions indicated that one of the 3-substituted heptose units was totally substituted at position C-7 from a terminal non-reducing heptose, definitively confirming the presence of the entirely insertion of the heptose III. However, restoring of wild type LPS structure did not change the OMPs aggregation tendency observed in *E. coli* S17-1(λ*pir*), as showed in Fig. 1 by the presence of OMPs inclusion bodies even in the recombinant cells.

The detailed structural determination of LPS in *E. coli* S17-1(λ*pir*) demonstrated that there is not an influence of LPS on the OMPs inclusion bodies formation. On this ground we would suggest the occurrence of another mutation, arisen during strain developed, that justify the OMPs aggregation phenotype we described.

Sequencing of this strain is currently under work with the aim to find some significant mutation. In any case the present evidences contribute to the still open debate on the LPS involvement in OMPs biogenesis, supporting the idea of independence of OMP biogenesis from LPS structure.

FUNDING

German Research Foundation, (DFG grant LI-448/4-1 to B.L.) in part; Ministero dell'Università e della Ricerca Scientifica (Progetti di Rilevante Interesse Nazionale 2006, Progetti di Rilevante Interesse Nazionale 2007).

CONFLICT OF INTEREST

None declared.

REFERENCES

1. Bernstain, H. (2000) The biogenesis and assembly of bacterial membrane proteins. *Curr. Opin. Microbiol.* **5**, 203–209
2. Paetzel, M., Dalbey, R.E., and Strynadka, N.C. (2000) The structure and mechanism of bacterial type I signal peptidases. A novel antibiotic target. *Pharmacol. Ther.* **87**, 27–49
3. Surrey, T. and Jähnig, F. (1995) Kinetics of folding and membrane insertion of a beta-barrel membrane protein. *J. Biol. Chem.* **270**, 28199–28203
4. Walton, T.A. and Sousa, M.C. (2004) Crystal structure of Skp, a prefoldin-like chaperone that protects soluble and membrane proteins from aggregation. *Mol. Cell.* **15**, 367–374
5. Bitto, E. and McKay, D.B. (2002) Crystallographic structure of SurA, a molecular chaperone that facilitates folding of outer membrane porins. *Structure.* **10**, 1489–1498
6. Mogensen, J.E. and Otzen, D.E. (2005) Interactions between folding factors and bacterial outer membrane proteins. *Mol. Microbiol.* **57**, 326–346
7. Voulhoux, R. and Tommassen, J. (2004) Omp85, an evolutionarily conserved bacterial protein involved in outer membrane-protein assembly. *Res. Microbiol.* **155**, 129–135
8. Voulhoux, R., Bos, M.P., Geurtsen, J., Mols, M., and Tommassen, J. (2003) Role of a highly conserved bacterial protein in outer membrane protein assembly. *Science* **299**, 262–265
9. Bogdanov, M. and Dowhan, W. (1999) Lipid-assisted protein folding. *J. Biol. Chem.* **274**, 36827–36830
10. de Cock, H., Pasveer, M., Tommassen, J., and Bouveret, E. (2001) Identification of phospholipids as new components that assist in the in vitro trimerization of a bacterial pore protein. *Eur. J. Biochem.* **268**, 865–875
11. Laird, M.W., Kloser, A.W., and Misra, R. (1994) Assembly of LamB and OmpF in deep rough lipopolysaccharide mutants of Escherichia coli K-12. *J. Bacteriol.* **176**, 2259–2264
12. Ferguson, A.D., Welte, W., Hofmann, E., Lindner, B., Holst, O., Coulton, J.W., and Diederichs, K. (2000) A conserved structural motif for lipopolysaccharide recognition by prokaryotic and eucaryotic proteins. *Structure Fold. Des.* **8**, 585–592
13. Vandeputte-Rutten, L., Kramer, R.A., Kroon, J., Dekker, N., Egmond, M.R., and Gros, P. (2001) Crystal structure of the outer membrane protease OmpT from Escherichia coli suggests a novel catalytic site. *EMBO J.* **20**, 5033–5039
14. de Cock, H. and Tommassen, J. (1996) Lipopolysaccharides and divalent cations are involved in the formation of an assembly-competent intermediate of outer-membrane protein PhoE of E. coli. *EMBO J.* **15**, 5567–5573
15. de Cock, H., Brandenburg, K., Wiese, A., Holst, O., and Seydel, U. (1999) Non-lamellar structure and negative charges of lipopolysaccharides required for efficient folding of outer membrane protein PhoE of Escherichia coli. *J. Biol. Chem.* **274**, 5114–5119
16. Bulieris, P.V., Behrens, S., Holst, O., and Kleinschmidt, J.H. (2003) Folding and insertion of the outer membrane protein OmpA is assisted by the chaperone Skp and by lipopolysaccharide. *J. Biol. Chem.* **278**, 9092–9099
17. Bos, M.P. and Tommassen, J. (2004) Biogenesis of the Gram-negative bacterial outer membrane. *Curr. Opin. Microbiol.* **7**, 610–616
18. Steeghs, L., de Cock, H., Evers, E., Zomer, B., Tommassen, J., and van der Ley, P. (2001) Outer membrane

composition of a lipopolysaccharide-deficient Neisseria meningitidis mutant. *EMBO J.* **20**, 6937–6945
19. Yethon, J.A., Heinrichs, D.E., Monteiro, M.A., Perry, M.B., and Whitfield, C. (1998) Involvement of wwaY, waaQ, and waaP in the modification of Escherichia coli lipopolysaccharide and their role in the formation of a stable outer membrane. *J. Biol. Chem.* **273**, 26310–26316
20. Sambrook, J., Fritsch, E.F., and Maniatis, T. (1989) *Molecular Cloning: A Laboratory Manual*, 2nd edn, pp. 1339–1341, Cold Spring Harbor Laboratory, Cold Spring Harbor, NY
21. Galanos, C., Lüderitz, O., and Westphal, O. (1969) A new method for the extraction of R lipopolysaccharides. *Eur. J. Biochem.* **9**, 245–249
22. Ciucanu, I. and Kerek, F. (1984) A simple and rapid method for the permethylation of carbohydrates. *Carbohydr. Res.* **131**, 209–217
23. Forsberg, L.S., Ramadas Bhat, U., and Carlson, R.W. (2000) Structural characterization of the O-antigenic polysaccharide of the lipopolysaccharide from Rhizobium etli strain CE3. *J. Biol. Chem.* **275**, 18851–18863
24. Leontein, K., Lindberg, B., and Lönngren, J. (1978) Assignment of absolute configuration of sugars by g.l.c. of their acetylated glycosides from chiral alcohols. *Carbohydr. Res.* **62**, 359–362
25. Singh, S.M. and Panda, A.K. (2005) Solubilization and refolding of bacterial inclusion body proteins. *J. Biosci. Bioeng.* **99**, 303–310
26. Simon, R., Priefer, U., and Pühler, A. (1983) A broad host range mobilization system for in vivo genetic engineering: transposon mutagenesis in gram negative bacteria. *Biotechnology* **1**, 784–791
27. Bachmann, B.J. (1987) Derivations and genotypes of some mutant derivatives of Escherichia coli K-12 in *Escherichia coli and Salmonella: Cellular and Molecular Biology* (Ingraham, J.L. and Neidhardt, F.C., eds.), pp. 1190–1219, ASM Press, USA
28. Tascon, R., Rodriguez-Ferri, E.F., Gutierrez-Martin, C.B., Rodriguez-Barbosa, I., Berche, P., and Vazquez-Boland, J.A. (1993) Transposon mutagenesis in Actinobacillus pleuropneumoniae with a Tn10 derivative. *J. Bacteriol.* **175**, 5717–5722
29. Kleinschmidt, J. H. (2003) Membrane protein folding on the example of outer membrane protein A of Escherichia coli. *Cell. Mol. Life Sci.* **60**, 1547–1558
30. Koebnik, R., Locher, K. P., and Van Gelder, P. (2000) Structure and function of bacterial outer membrane proteins: barrels in a nutshell. *Mol. Microbiol.* **37**, 239–253
31. Basle, A., Rummel, G., Storici, P., Rosenbusch, J. P., and Schirmer, T. (2006) Crystal structure of osmoporin OmpC from E. coli at 2.0 A. *J. Mol. Biol.* **362**, 933–942
32. Sen, K. and Nikaido, H. (1991) Trimerization of an in vitro synthesized OmpF porin of Escherichia coli outer membrane. *J. Biol. Chem.* **266**, 11295–1130025
33. Castillo Keller, M. and Misra, R. (2003) Protease-deficient DegP suppresses lethal effects of a mutant OmpC protein by its capture. *J. Bacteriol.* **185**, 148–154
34. Reid, J., Fung, H., Gehring, K., Klebba, P. E., and Nikaido, H. (1988) Targeting of porin to the outer membrane of Escherichia coli. Rate of trimer assembly and identification of a dimer intermediate. *J. Biol. Chem.* **263**, 7753–7759
35. Watanabe, Y. (2002) Effect of various mild surfactants on the reassembly of an oligomeric integral membrane protein OmpF porin. *J. Protein. Chem.* **21**, 169–175
36. Visudtiphole, V., Thomas, M.B., Chalton, D.A., and Lakey, J.H. (2005) Refolding of Escherichia coli outer membrane protein F in detergent creates LPS-free trimers and asymmetric dimers. *Biochem. J.* **392**, 375–381
37. Zähringer, U., Lindner, B., and Rietschel, E. T. (1999) Chemical structure of lipid A: recent advances in structural analysis of biologically active molecules in *Endotoxin in Health and Disease* (Brade, H., Opal, S. M., Vogel, S. N., and Morrison, D. C., eds.), pp. 93–114, Marcel Dekker, Inc., New York, Basel
38. Lipkind, G.M., Shashkov, A.S., Knirel, Y.A., Vinogradov, E.V., and Kochetkov, N.K. (1988) A computer-assisted structural analysis of regular saccharides on the basis of 13C-NMR data. *Carbohydr. Res.* **175**, 59–75
39. Müller-Loennies, S., Lindner, B., and Brade, H. (2003) Structural analysis of oligosaccharides from lipopolysaccharide (LPS) of Escherichia coli K-12 strain W3100 reveals a link between inner and outer core LPS biosynthesis. *J. Biol. Chem.* **278**, 34090–101
40. Mahillon, J. and Chandler, M. (1998) Insertion sequences. *Microbiol. Mol. Biol. Rev.* **62**, 725–774
41. Clementz, T. (1992) The gene coding for 3-deoxy-manno-octulosonic acid transferase and the rfaQ gene are transcribed from divergently arranged promoters in Escherichia coli. *J. Bacteriol.* **174**, 7750–7756
42. Yanisch-Perron, C., Vieira, J., and Messing, J. (1985) Improved M13 phage cloning vectors and host strains: nucleotide sequences of the M13mpl8 and pUC19 vectors. *Gene.* **33**, 103–109